AGU PUBLICATIONS

Geophysical Research Letters

RESEARCH LETTER
10.1002/2015GL066599

Key Points:
- Plasma density, deduced from spacecraft potential, traces neutral density, implying local ionization
- We determine the plasma density increase due to decreased heliocentric distance and seasonal effects
- Low collision rate keeps the electron temperature high (~5 eV), giving a negative spacecraft potential

Correspondence to:
E. Odelstad,
elias.odelstad@irfu.se

Citation:
Odelstad, E., A. I. Eriksson, N. J. T. Edberg, F. Johansson, E. Vigren, M. André, C.-Y. Tzou, C. Carr, and E. Cupido (2015), Evolution of the plasma environment of comet 67P from spacecraft potential measurements by the Rosetta Langmuir probe instrument, *Geophys. Res. Lett.*, *42*, 10,126–10,134, doi:10.1002/2015GL066599.

Received 15 OCT 2015
Accepted 20 NOV 2015
Accepted article online 24 NOV 2015
Published online 11 DEC 2015

Evolution of the plasma environment of comet 67P from spacecraft potential measurements by the Rosetta Langmuir probe instrument

E. Odelstad[1,2], A. I. Eriksson[1], N. J. T. Edberg[1], F. Johansson[1], E. Vigren[1], M. André[1], C.-Y. Tzou[3], C. Carr[4], and E. Cupido[4]

[1]Swedish Institute of Space Physics, Uppsala, Sweden, [2]Department of Physics and Astronomy, Uppsala University, Uppsala, Sweden, [3]Physikalisches Institut, Universität Bern, Bern, Switzerland, [4]Space and Atmospheric Physics Group, Imperial College, London, UK

Abstract We study the evolution of the plasma environment of comet 67P using measurements of the spacecraft potential from early September 2014 (heliocentric distance 3.5 AU) to late March 2015 (2.1 AU) obtained by the Langmuir probe instrument. The low collision rate keeps the electron temperature high (~5 eV), resulting in a negative spacecraft potential whose magnitude depends on the electron density. This potential is more negative in the northern (summer) hemisphere, particularly over sunlit parts of the neck region on the nucleus, consistent with neutral gas measurements by the Cometary Pressure Sensor of the Rosetta Orbiter Spectrometer for Ion and Neutral Analysis. Assuming constant electron temperature, the spacecraft potential traces the electron density. This increases as the comet approaches the Sun, most clearly in the southern hemisphere by a factor possibly as high as 20–44 between September 2014 and January 2015. The northern hemisphere plasma density increase stays around or below a factor of 8–12, consistent with seasonal insolation change.

1. Introduction

Comets are small solar system bodies consisting of a mixture of volatile and refractory materials, which were left over after the formation of the outer planets. The volatiles are dominated by H_2O, CO, and CO_2 [*Bockelée-Morvan et al.*, 2004; *Hässig et al.*, 2015], partly released from the nucleus when insolation increases as a comet enters the inner solar system . This gas, and the refractory dust that it entrains, forms a coma enveloping the comet nucleus. Photoionization of the neutral gas by solar extreme ultraviolet radiation, as well as charge exchange and electron impact reactions with the solar wind and high-energy electrons, combines to produce a cometary ionosphere [*Combi et al.*, 2004], with a dust component charged by the competing effects of photoelectron emission and attaching plasma electrons.

The Rosetta spacecraft arrived at comet 67P/Churyumov-Gerasimenko (hereafter 67P) in August 2014. Previous space missions to comets have all been rapid flybys at large distances ($\gtrsim$600 km) near perihelion. Rosetta's prolonged stay at distances ~10–100 km from the comet nucleus offers an unprecedented opportunity to study the evolution of the near-nucleus plasma environment from a heliocentric distance of 3.6 AU at the 6 August 2014 rendezvous, to the comet perihelion at 1.24 AU in August 2015. The spacecraft carries a five instrument suite for plasma and electric field measurements, the Rosetta Plasma Consortium (RPC) [*Carr et al.*, 2007], including the Langmuir probe instrument (RPC-LAP) [*Eriksson et al.*, 2007] we use in this study.

The shape and rotational state of 67P have been determined by Rosetta's Optical, Spectroscopic and Infrared Remote Imaging System (OSIRIS), showing a two lobe nucleus rotating with a period of ~12.4 h [*Sierks et al.*, 2015]. The northern hemisphere of the nucleus was experiencing summer, being subject to more solar illumination than the southern (winter) hemisphere, until equinox in May 2015.

OSIRIS also detected the presence of a dust coma, with activity predominantly from the neck region connecting the two lobes of the nucleus [*Sierks et al.*, 2015]. Observations of water vapor by the Microwave Instrument on the Rosetta Orbiter showed periodic peaks in production rate coinciding with solar illumination of the neck region, where also the largest column densities were observed [*Gulkis et al.*, 2015]. The total water production

rate was inferred to have increased from $1 \cdot 10^{25}$ molecules/s in early June 2014 to $4 \cdot 10^{25}$ molecules/s in late August of that year. Measurements by the Visible, Infrared and Thermal Imaging Spectrometer from late November 2014 to late January 2015 similarly showed elevated water column densities above the neck region, while the water production rate was found to be almost constant at approximately $8 \cdot 10^{25}$ molecules/s during this time period [*Bockelée-Morvan et al.*, 2015]. The Rosetta Orbiter Spectrometer for Ion and Neutral Analysis (ROSINA) found an increase of the coma density during the approach phase in August 2014 that roughly corresponded to a $1/r^2$ dependence on cometocentric distance for the main constituents, H_2O, CO, and CO_2 [*Hässig et al.*, 2015]. Peaks in the H_2O and CO signals were observed when the neck region was in view of the spacecraft, and there was a deep minimum in the H_2O signal at negative latitudes in the winter hemisphere, where CO_2 was more prominent.

Plasma of cometary origin has been observed by the Ion Composition Analyzer (RPC-ICA) since 7 August 2014, at a distance of 100 km from the nucleus, in the form of water ions picked up by the solar wind electric field and accelerated toward the spacecraft perpendicular to the solar wind direction [*Nilsson et al.*, 2015a]. Locally produced water ions, accelerated into the instrument by a negative spacecraft potential, were first detected by the Rosetta Ion and Electron Sensor (RPC-IES) on 19 August 2014 at a distance of ~80 km from the nucleus [*Goldstein et al.*, 2015]. These ions have also been detected by RPC-ICA, starting on 21 September 2014 at a distance of 28 km from the nucleus. At this time, there was also a detectable deflection of the solar wind due to mass loading resulting from the ion pickup process. Plasma densities were estimated to be in the range 1–10 cm^{-3}, with ion drift velocities on the order of 1–10 km/s [*Nilsson et al.*, 2015a]. Thus, at 28 km from the nucleus and a heliocentric distance of ~3.3 AU, the cometary plasma was found to be similar in number density to that of the solar wind, indicating the emergence of a cometary ionosphere that was beginning to repel the solar wind. The average flux of water pickup ions increased by as much as 4 orders of magnitude between early August 2014 and late March 2015 (corresponding to heliocentric distances from 3.6 to 2.0 AU) [*Nilsson et al.*, 2015b].

In the current study, we focus on the low-energy locally produced plasma detectable by RPC-LAP. *Edberg et al.* [2015] mapped the near-nucleus spatial distribution of this plasma using RPC-LAP during a 2 week period in October 2014 when Rosetta was at a cometocentric distance of ~10 km (heliocentric distance ~3.1 AU), finding a highly structured plasma environment with the highest density in the summer hemisphere and above the neck region of the comet. Altitude profiles from two flybys in February were consistent with a $1/r$ dependence of plasma density on cometocentric distance, at least within 260 km of the nucleus. In the present study, we follow the evolution of this plasma as comet activity increases from early September 2014 (3.5 AU) to late March 2015 (2.1 AU).

2. Instrumentation and Measurements

Our main data source is the RPC-LAP instrument, which we concentrate on here. For context, we also use neutral gas densities from the ROSINA Cometary Pressure Sensor (COPS), described by, e.g., *Hässig et al.* [2015], *Bieler et al.* [2015], *Balsiger et al.* [2007], and references therein.

The RPC-LAP instrument consists of two spherical Langmuir probes (denoted LAP1 and LAP2) of 2.5 cm radius, mounted on 15 cm stubs on the tips of booms of length 2.24 m and 1.62 m, respectively. The longer boom, on which LAP1 is mounted, is directed at an angle of 45° to the nominal nucleus direction, providing access to plasma flow from the comet with the least amount of disturbances by spacecraft sheath or wake effects that is possible while respecting the field of view of other instruments. This positioning puts LAP1 in sunlight under nominal pointing conditions when the spacecraft is in near-terminator orbit around the comet, which was the most common orbital configuration during the early science phase of the mission.

The measurements used in this paper were obtained using LAP1 bias voltage sweeps, recording the probe current as the bias voltage to the probe is varied. The resulting current-voltage relationship can be compared to theoretical models to produce estimates of electron density and temperature, ion density and flow speed, spacecraft potential $V_{S/C}$, and mean ion mass and integrated UV flux [*Eriksson et al.*, 2007; *Mott-Smith and Langmuir*, 1926]. Density and temperature estimates from automated analysis of such sweeps over long time periods in the highly variable and evolving environment is difficult. However, consistent and reliable estimates of the spacecraft potential $V_{S/C}$ have been obtained from such an analysis. Hence, in this study we focus on the evolution of $V_{S/C}$ and what it reveals about the evolution of the cometary plasma environment.

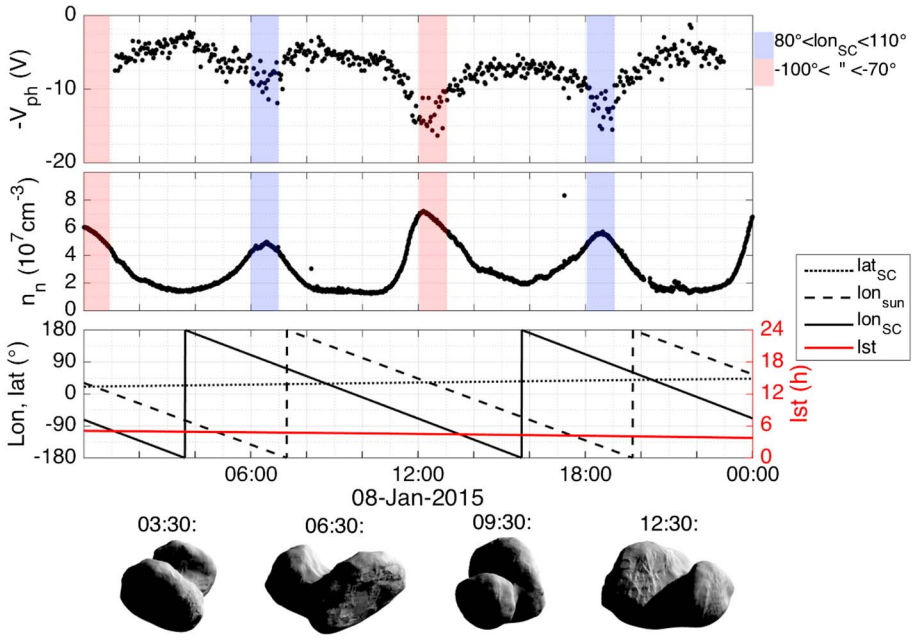

Figure 1. (upper) RPC-LAP spacecraft potential and (middle) ROSINA-COPS neutral gas density measurements, taken on 8 January 2015, at 28 km from the nucleus. (bottom) Latitude and longitude of the spacecraft and the longitude of the Sun, in comet-fixed coordinates, as well as the local solar time. Blue and red colored patches indicate times when the longitude of the spacecraft was between 80° and 110° and −100° and −70°, respectively. Spacecraft perspectives of the partially illuminated nucleus are shown for four different times below the bottom panel.

In addition, $V_{S/C}$ regulates, e.g., possibilities to detect low-energy ions [*Nilsson et al.*, 2015b] and charged dust [*Fulle et al.*, 2015], as, e.g., a negative $V_{S/C}$ accelerates positive particles toward the detector and completely rejects negatively charged particles with energy per charge below $|V_{S/C}|$.

Our $V_{S/C}$ estimates are obtained by finding the highest probe bias voltage at which a sunlit probe still emits all its photoelectrons, V_{ph}. Once the probe potential becomes positive with respect to the surrounding plasma, photoelectrons will begin to be attracted back to the probe, and the photoemission current decreases rapidly with increasing probe potential. This gives rise to a sharp inflection point in the current-voltage relationship, viz., the photoelectron knee, that can be identified in the sweeps [*Eriksson et al.*, 2007]. The bias potential at which this knee occurs is equal to the potential, with respect to the spacecraft, of the plasma in which the probe is immersed. Thus, an estimate of the spacecraft potential can be obtained by simply changing the sign of the photoelectron knee potential V_{ph}.

Since the charged spacecraft perturbs the potential of the surrounding plasma and the boom length is smaller than or comparable to the Debye length (~1–10 m for the studied time period [*Edberg et al.*, 2015]), the plasma potential at the probe will in general not be the same as that of the unperturbed plasma far away from the spacecraft. Simulations indicate that, for LAP1 in a tenuous solar wind environment, the ratio $V_{ph}/V_{S/C}$ is on the order of −1/2 to −2/3 [*Sjogren et al.*, 2012]. Though values closer to −1 are expected for shorter Debye lengths in denser plasmas, these values are roughly in agreement with initial comparisons to RPC-ICA (not shown). In the following we will neglect this correction factor, as the evolution of the plasma environment can be equally well followed by the observable V_{ph}.

3. Spacecraft Potential as a Monitor of the Cometary Plasma Environment

For the plasma conditions relevant here, $V_{S/C}$ is set by the balance of currents due to emission of photoelectrons from the spacecraft and collection of ambient plasma electrons [*Pedersen*, 1995]. When the spacecraft is negatively charged, the current due to plasma electrons is

$$I_e = A_{S/C} n_e e \frac{v_{\mathrm{th}}}{2} \exp\left\{\frac{eV_{S/C}}{k_B T_e}\right\}, \quad (1)$$

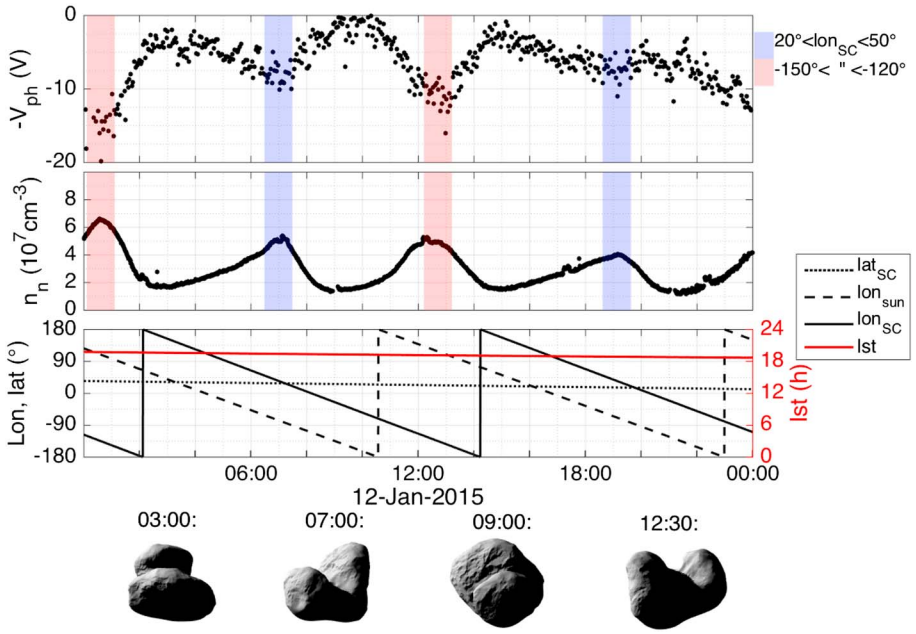

Figure 2. (upper) RPC-LAP spacecraft potential and (middle) ROSINA-COPS neutral gas density measurements, taken on 12 January 2015, at 28 km from the nucleus. (bottom) Latitude and longitude of the spacecraft and the longitude of the Sun, in comet-fixed coordinates, as well as the local solar time. Blue and red colored patches indicate times when the longitude of the spacecraft was between 20° and 50° and −150° and −120°, respectively. Spacecraft perspectives of the partially illuminated nucleus are shown for four different times below the bottom panel.

where $n_{e,s/c}$ is the electron density in the surrounding plasma, e is the elementary charge and the thermal speed, defined as the mean of the magnitude of the velocity in any one dimension, is $v_{th}=\sqrt{2k_BT_e/\pi m_e}$, where k_B is Boltzmann's constant, T_e is the electron temperature and m_e is the electron mass. $A_{S/C}$ is the total current-collecting area of the spacecraft, including the solar panels which have conducting surfaces and are connected to spacecraft ground. Equating I_e with the spacecraft photoemission current I_{ph}, which is independent of $V_{S/C}$ for a negatively charged spacecraft, and solving for $V_{S/C}$ gives

$$V_{S/C} = -\frac{k_B T_e}{e} \log\left\{\frac{A_{S/C} n_e e v_{th}/2}{I_{ph}}\right\}. \quad (2)$$

Thus, the spacecraft potential can be used to monitor the plasma environment of the comet, with a more negative spacecraft potential indicating higher electron fluxes ($\propto n_e\sqrt{T_e}$) in the plasma. The electron density and temperature cannot be disentangled by this method but for the purpose of this study we will generally attribute any variations in $V_{S/C}$ to changes in n_e, assuming a constant T_e of 5 eV, which is supported by initial analysis of the LAP sweep measurements. Also, the consistency of the negative $V_{S/C}$ shows that variations in T_e must be much smaller than the variations of n_e, which can be several orders of magnitude [*Edberg et al.*, 2015].

4. Observations

Figure 1 shows an example of spacecraft potential measurements (upper panel), taken on 8 January 2015, when Rosetta was in near-terminator orbit at 28 km from the nucleus. We plot the negative of the photoelectron knee potential $-V_{ph}$, noting that the actual value of $V_{S/C}$ may be up to a factor $\alpha \sim 1.5 - 2$ larger. Latitude and longitude of the spacecraft in the Cheops reference frame [*Preusker et al.*, 2015] are shown in the bottom panel, together with the longitude of the Sun and the local solar time (red curve, to be read off the right-hand y axis). Local solar time (lst) was about 5 h, so the spacecraft was on the dawnside of the nucleus. $-V_{ph}$ was consistently negative during this day, generally ranging between −2 V and −16 V, with recurring dips every 6 hours, corresponding to half the rotation period of the nucleus. These dips coincide with peaks in the neutral gas density observed by COPS (middle panel) and can be attributed to two distinct longitude intervals, [80°, 110°] and [−100°, −70°], marked in Figure 1 by blue and red patches, respectively.

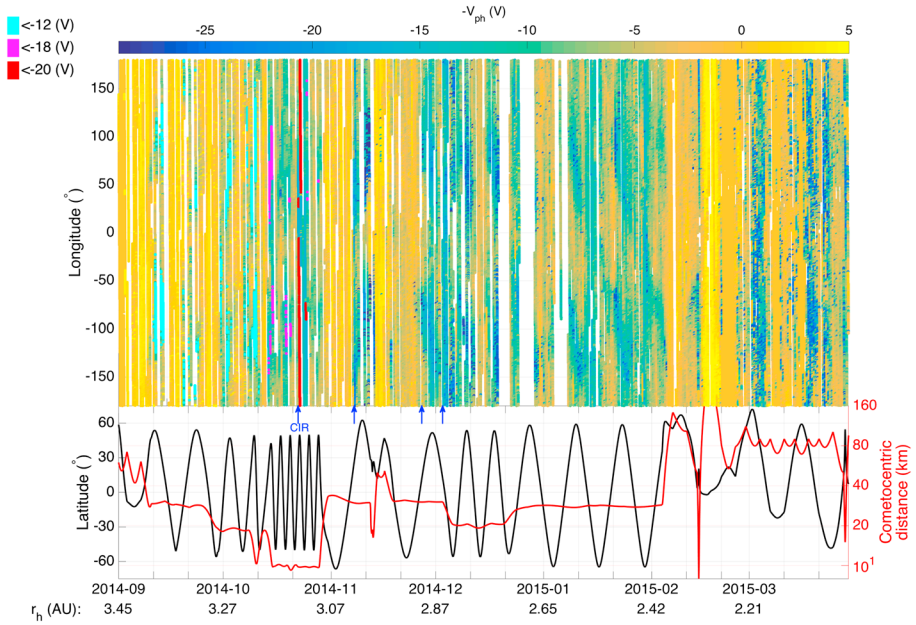

Figure 3. Overview of RPC-LAP spacecraft potential measurements from early September 2014 to late March 2015. (top) The negative of the photoelectron knee potential color coded on a time-longitude map. (bottom) The latitude in black (to be read off the left-hand vertical axis) and the cometocentric distance in red (right-hand vertical axis). Cyan, magenta and red colors indicate measurements where the negative of the photoelectron knee potential went below the measurement range of −12 V, −18 V, or −20 V, respectively. Blue arrows indicate times of CIR impacts, see text.

Spacecraft perspectives of the partially illuminated nucleus, generated from a shape model based on OSIRIS images [*Preusker et al.*, 2015], are shown for four different times at the bottom of Figure 1. The peaks in neutral gas density and the coincident dips in spacecraft potential occur when sunlit parts of the neck region of the nucleus are in view of the spacecraft.

Figure 2 shows another example of spacecraft potential measurements, taken on 12 January 2015, also at a distance of 28 km from the nucleus and passing through similar latitudes and longitudes as in Figure 1. However, this time the spacecraft was on the dusk side of the comet, the local solar time being about 18 h. The spacecraft potential still traces the neutral gas density, whose peaks have now shifted to the longitude intervals [20°, 50°] and [−150°, −120°], respectively. The peaks still occur when sunlit parts of the neck region are in view of the spacecraft, but the longitudes where this happens have changed since the illumination of the nucleus is different on the dusk side.

Figure 3 (top) shows an overview of $V_{S/C}$ from early September 2014 to late March 2015, scatterplotted versus time on the horizontal axis, longitude on the vertical axis and with each point color coded by $-V_{ph}$. Figure 3 (bottom) shows the latitude in black and the cometocentric distance in red (to be read off the left-hand and right-hand vertical axes, respectively). The voltage range swept by the Langmuir probe varied between different measurement modes. In September and October it was typically −12 V to +12 V or −18 V to +18 V, except during shorter periods of higher telemetry rate when it was −30 V to +20 V. Occasionally, V_{ph} would become larger than the upper edge of the sweep bias range; for these cases we use this upper edge as a lower limit. In Figure 3, such limit values are color coded by cyan, magenta, or red for maximum sweep potentials of +12 V, +18 V, and +20 V, respectively. From late October, the sweeps typically ran all the way up to +30 V, the maximum the instrument can produce.

The spacecraft was negatively charged most of the time during the plotted period, only reaching positive potentials at distances $\gtrsim$50 km in the southern hemisphere in early September and during the excursion out to distances beyond 150 km in late February. In general, the spacecraft went more negative in the northern (summer) hemisphere than in the southern (winter) hemisphere, attributable to seasonal differences. The periodic dips in spacecraft potential observed in Figures 1 and 2 are ubiquitous features in the northern hemisphere, consistent with higher densities above the neck region of the nucleus. There is also a strong radial dependence with more negative spacecraft potentials observed closer to the comet, as expected

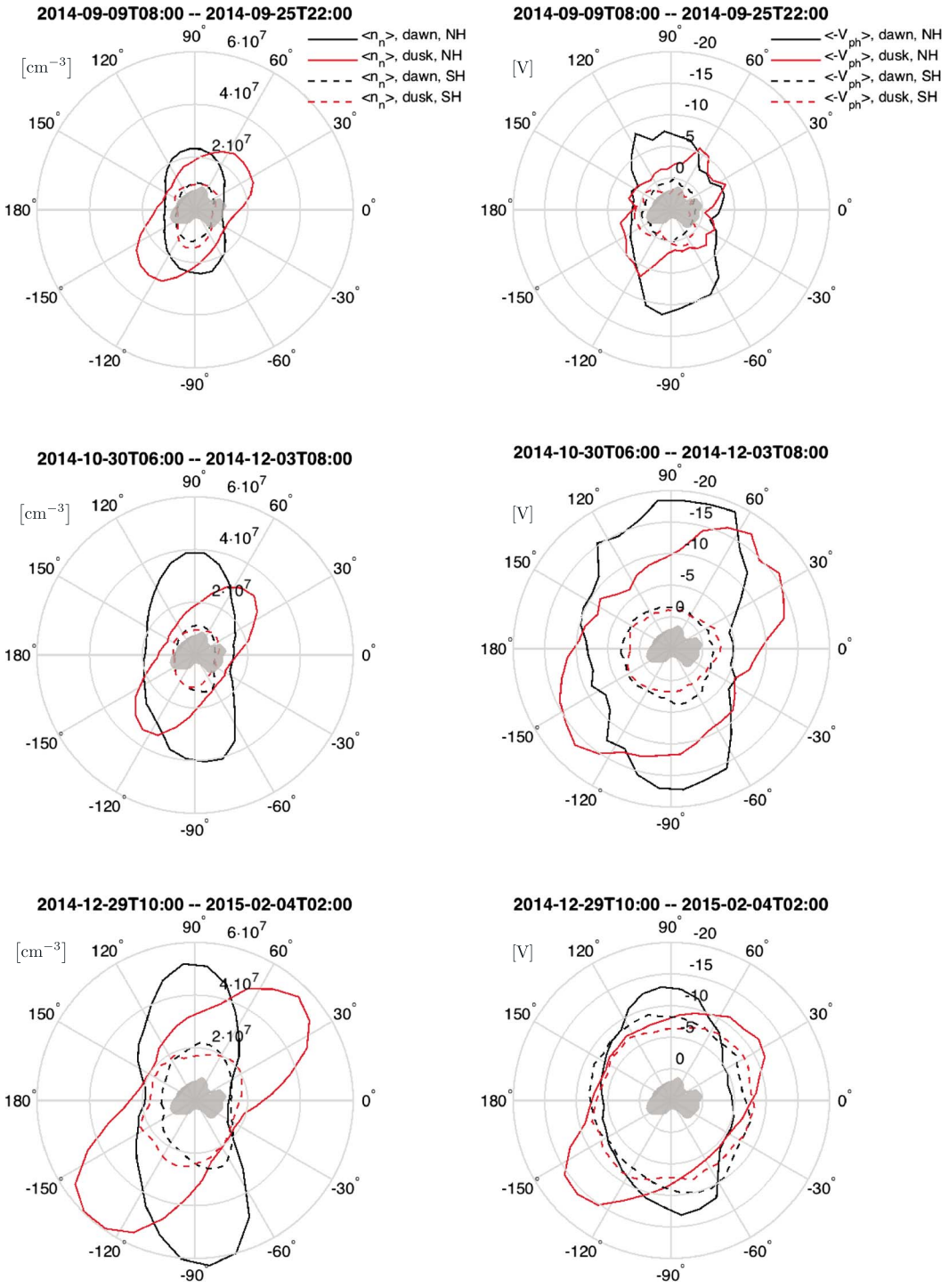

Figure 4. (left column) Radial plots of ROSINA-COPS neutral densities and (right column) RPC-LAP spacecraft potentials averaged over 10° longitude bins for the three time intervals at ~30 km in September 2014, November 2014, and January 2015, respectively. The data have been sorted by acquisition hemisphere (solid curves for northern hemisphere and dashed curves for southern hemisphere) and local solar time (black curves for dawn and red curves for dusk).

due to the density decaying with cometocentric distance. A general trend toward more negative spacecraft potentials with decreasing heliocentric distance can also be seen, indicative of increasing comet activity.

Several impacts of solar wind disturbances known as corotating interaction regions (CIRs) have been identified in the data, including 22 October 2014, 7 and 27 November 2014, and 3 December 2014 (Edberg et al., Solar wind interaction with comet 67P: Impacts of corotating interaction regions, submitted to *Journal of Geophysical Research*, 2015), marked by blue arrows in Figure 3. All of these are dates when we see conspicuous drops in the spacecraft potential (Figure 3). This shows that the cometary plasma environment is sensitive also to variations in the solar wind conditions, so all details in Figure 3 should not be interpreted as variations of the comet activity.

To more clearly bring out the long term evolution of the plasma environment and disentangle it from the effects of radial distance, latitude and longitude, we single out the three time intervals in September, November, and January, respectively, during which the spacecraft was consistently at ∼30 km from the nucleus. Figure 4 shows the average of the neutral gas density (left column) and $-V_{\mathrm{ph}}$ (right column) over 10° longitude bins in the northern (solid curves) and southern (dashed curves) hemispheres, respectively, for each of the three time intervals. We also separate data from the dawn and dusk sides of the nucleus (black and red curves, respectively). Clearly unphysical peaks in the neutral gas density have been removed by rejecting values above $3 \cdot 10^7$ cm^{-3} in the northern hemisphere during the September and January intervals, $4.5 \cdot 10^7$ cm^{-3} in the southern hemisphere during the September interval, and 10^8 cm^{-3} in the northern hemisphere during the November interval and both hemispheres during the January interval. For the November interval, in the middle of which the cometocentric distance varied greatly in connection with the lander delivery, only data obtained at distances between 27 and 33 km have been included. For all three time intervals, the previously mentioned latitude and longitude dependences, as well as the asymmetry between the dawn and dusk sides in the coma, are observed with clarity in both the neutral gas density and spacecraft potential. In the southern hemisphere, $-V_{\mathrm{ph}}$ decreased by ∼2–3 V between the September and November intervals and by another 5–6 V between the November and January intervals. In the northern hemisphere, the average of $-V_{\mathrm{ph}}$ decreased by 7.5 V between the September and November intervals and then increased by 2.7 V between the November and January intervals. The conspicuously large negative potentials in the northern hemisphere during the November interval are likely due to increased flux of high-energy (∼100 eV) electrons seen by the Ion and Electron Sensor (RPC-IES) [*Clark et al.*, 2015], possibly related to the CIR impacts on 7 and 27 November. Such high-energy electrons can have a disproportionately large contribution to the spacecraft potential and may also contribute to an increased ionization rate [*Clark et al.*, 2015]. Seasonal effects cannot explain this feature in the data since even though the total sunward projected area in the northern hemisphere of the nucleus decreased between November and January, the increased sunlight intensity due to the $1/r^2$ dependence on heliocentric distance was much larger and there was a net increase in insolation even in this hemisphere. This is corroborated by the fact that the neutral gas density as observed by ROSINA/COPS is not higher in the November interval than in January.

5. Discussion

Generally speaking, we attribute decreases in the spacecraft potential to increases of the electron density in the surrounding plasma, provisionally ignoring the possible effects of variations in the electron temperature . Thus, the above observations suggest that there is more plasma above the northern hemisphere, in line with the neutral gas observations by ROSINA [*Hässig et al.*, 2015]. This is also consistent with northern summer in this period. The dips in spacecraft potential above the neck region of the comet indicate a further increase in plasma density there, also consistent with the neutral gas observations.

A tentative quantification of the increase in plasma density can be obtained under the assumption of constant electron temperature. Solving for n_e in equation (2) gives

$$n_e = \frac{I_{\mathrm{ph}}}{A_{S/C} e v_{\mathrm{th}}/2} \exp\left\{-\frac{eV_{S/C}}{k_B T_e}\right\}; \tag{3}$$

hence, a change $\Delta V_{S/C}$ of the spacecraft potential implies a relative change in electron density

$$\frac{n_{e2}}{n_{e1}} = \frac{I_{\mathrm{ph},2}}{I_{\mathrm{ph},1}} \exp\left\{-\frac{e\Delta V_{S/C}}{k_B T_e}\right\}, \tag{4}$$

where $I_{ph,2}/I_{ph,1}$ is the relative change in spacecraft photoemission current. Assuming a $1/r^2$ dependence on heliocentric distance gives $I_{ph,2}/I_{ph,1} \sim 1.4$ between the September and November intervals and $I_{ph,2}/I_{ph,1} \sim 1.3$ between the November and January intervals, the heliocentric distances being about 3.4 AU, 3.0 AU, and 2.5 AU, respectively. This also agrees relatively well with the observed evolution of the photoemission current of LAP1 as observed from the current jumps at negative bias potentials when the probe comes into and out of shadow (not shown). Assuming a constant T_e of 5 eV, equation (4) then gives an increase of n_e in the southern hemisphere by a factor of ~3–4 from September to November and ~7–12 from November to January, for values of α of 1.5–2. In the northern hemisphere, the same calculations are potentially deceptive since the spacecraft potential in November was likely influenced by the effects of suprathermal electrons that are not accounted for in the above model. A comparison between the September and January intervals suggests an increase of n_e in the northern hemisphere by a factor of ~8–12.

The assumption of a constant electron temperature of 5 eV is highly provisional, based on an initial analysis of LAP sweep measurements, but the consistently negative $V_{S/C}$ values we find show that significant variations from this number must have been rare in the period of study. However, the above estimates of the increase in plasma density are very sensitive to the assumed electron temperature; e.g., a constant T_e of 10 eV would produce much lower values. Also, the evolution of the spacecraft potential presented in this paper is a convolution of changes in electron density and temperature, so some evolution toward lower T_e can be expected with increasing collisional cooling. This could possibly contribute to the spacecraft in the northern hemisphere being at a less negative potential in January than in November, although we expect this effect to be small since the average neutral gas density concurrently increased by only about 50%.

6. Summary and Conclusions

We have used measurements of the spacecraft potential obtained by the Rosetta Langmuir probe instrument to study the evolution of the plasma environment of comet 67P during the time period from early September 2014 to late March 2015, during which time the heliocentric distance decreased from about 3.5 AU to 2.1 AU and Rosetta's distance to the nucleus typically was between 10 and 150 km. The spacecraft potential was negative within 50 km of the nucleus throughout this period. We found a cometary plasma with a strong radial dependence and the highest densities (i.e., the most negative spacecraft potentials) observed in the northern (summer) hemisphere above the neck region of the comet nucleus, which is in line with what was observed by *Edberg et al.* [2015] during the 2 week period at ~10 km from the comet nucleus in October 2014. The exact longitudes at which the density peaks occurred were observed to vary between the dawnsides and dusksides of the comet, coinciding with sunlit parts of the neck region being in view of the spacecraft. In this regard, the plasma density was found to trace the neutral gas density. Whether this should be taken as evidence for elevated activity in the neck region of the nucleus is as yet unclear, since *Bieler et al.* [2015] found that an illumination-driven direct simulation Monte-Carlo model with a uniformly active surface was able to reproduce the ROSINA-COPS neutral density measurements when the complex nucleus shape and related illumination conditions were included.

A comparison between the time intervals at ~30 km cometocentric distance in September 2014, November 2014, and January 2015 showed increases in the estimated plasma density in the southern hemisphere by a factor of ~3–4 from September to November and ~7–12 from November to January, assuming a constant electron temperature of 5 eV. In the northern hemisphere the most negative spacecraft potentials were obtained during the November interval, but this coincided with an increased flux of suprathermal (~100 eV) electrons and is not interpreted as a surge in plasma density. Comparing the September and January intervals, the total increase in plasma density was estimated to be a factor of ~8–12 (also assuming $T_e = 5$ eV), which is less than in the southern hemisphere. This is presumably a result of the combination of the overall increase in insolation due to decreasing heliocentric distance and seasonal effects.

Acknowledgments

Rosetta is a European Space Agency (ESA) mission with contributions from its member states and the National Aeronautics and Space Administration (NASA). The work on RPC-LAP data was funded by the Swedish National Space Board under contracts 109/12, 135/13, and 166/14 and Vetenskapsrådet under contract 621-2013-4191. This work has made use of the AMDA and RPC Quicklook database, provided by a collaboration between the Centre de Donnees de la Physique des Plasmas (CDPP) (supported by CNRS, CNES, Observatoire de Paris and Universite Paul Sabatier, Toulouse), and Imperial College London (supported by the UK Science and Technology Facilities Council). Work at the University of Bern on ROSINA COPS was funded by the State of Bern, the Swiss National Science Foundation, and the European Space Agency PRODEX Program. We thank the OSIRIS team for making the comet shape model available. The data used in this paper will soon be made available on the ESA Planetary Science Archive and are available upon request until that time.

References

Balsiger, H., et al. (2007), Rosina Rosetta orbiter spectrometer for ion and neutral analysis, *Space Sci. Rev.*, *128*, 745–801, doi:10.1007/s11214-006-8335-3.

Bieler, A., et al. (2015), Comparison of 3D kinetic and hydrodynamic models to ROSINA-COPS measurements of the neutral coma of 67P/Churyumov-Gerasimenko, *Astron. Astrophys.*, *583*, A7, doi:10.1051/0004-6361/201526178.

Bockelée-Morvan, D., J. Crovisier, M. J. Mumma, and H. A. Weaver (2004), The composition of cometary volatiles, in *Comets II*, edited by M. Festou, H. U. Keller, and H. A. Weaver, pp. 391–423, Univ. of Arizona Press, Tucson, Ariz.

Bockelée-Morvan, D., et al. (2015), First observations of H_2O and CO_2 vapor in comet 67P/Churyumov-Gerasimenko made by VIRTIS onboard Rosetta, *Astron. Astrophys.*, *583*, A6, doi:10.1051/0004-6361/201526303.

Carr, C., et al. (2007), RPC: The Rosetta plasma consortium, *Space Sci. Rev.*, *128*, 629–647, doi:10.1007/s11214-006-9136-4.

Clark, G., et al. (2015), Suprathermal electron environment of comet 67P/Churyumov-Gerasimenko: Observations from the Rosetta Ion and Electron Sensor, *Astron. Astrophys.*, *583*, A24, doi:10.1051/0004-6361/201526351.

Combi, M. R., W. M. Harris, and W. H. Smyth (2004), Gas dynamics and kinetics in the cometary coma: Theory and observations, in *Comets II*, edited by M. C. Festou, H. U. Keller, and H. A. Weaver, pp. 523–552, Univ. of Arizona Press, Tucson, Ariz.

Edberg, N. J. T., et al. (2015), Spatial distribution of low-energy plasma around comet 67P/CG from Rosetta measurements, *Geophys. Res. Lett.*, *42*, 4263–4269, doi:10.1002/2015GL064233.

Eriksson, A. I., et al. (2007), RPC-LAP: The Rosetta Langmuir probe instrument, *Space Sci. Rev.*, *128*, 729–744, doi:10.1007/s11214-006-9003-3.

Fulle, M., et al. (2015), Density and charge of pristine fluffy particles from comet 67P/Churyumov-Gerasimenko, *Astrophys. J. Lett.*, *802*, L12, doi:10.1088/2041-8205/802/1/L12.

Goldstein, R., et al. (2015), The Rosetta Ion and Electron Sensor (IES) measurement of the development of pickup ions from comet 67P/Churyumov-Gerasimenko, *Geophys. Res. Lett.*, *42*, 3093–3099, doi:10.1002/2015GL063939.

Gulkis, S., et al. (2015), Subsurface properties and early activity of comet 67P/Churyumov-Gerasimenko, *Science*, *347*(6220), AAA0709, doi:10.1126/science.aaa0709.

Hässig, M., et al. (2015), Time variability and heterogeneity in the coma of 67P/Churyumov-Gerasimenko, *Science*, *347*(6220), AAA0276, doi:10.1126/science.aaa0276.

Mott-Smith, H. M., and I. Langmuir (1926), The theory of collectors in gaseous discharges, *Phys. Rev.*, *28*, 727–763, doi:10.1103/PhysRev.28.727.

Nilsson, H., et al. (2015a), Birth of a comet magnetosphere: A spring of water ions, *Science*, *347*(6220), AAA0571, doi:10.1126/science.aaa0571.

Nilsson, H., et al. (2015b), Evolution of the ion environment of comet 67P/Churyumov-Gerasimenko – Observations between 3.6 and 2.0 AU, *Astron. Astrophys.*, *583*, A20, doi:10.1051/0004-6361/201526142.

Pedersen, A. (1995), Solar wind and magnetosphere plasma diagnostics by spacecraft electrostatic potential measurements, *Ann. Geophys.*, *13*, 118–129, doi:10.1007/s00585-995-0118-8.

Preusker, F., et al. (2015), Shape model, reference system definition, and cartographic mapping standards for comet 67P/Churyumov-Gerasimenko – Stereo-photogrammetric analysis of Rosetta/OSIRIS image data, *Astron. Astrophys.*, *583*, A33, doi:10.1051/0004-6361/201526349.

Sierks, H., et al. (2015), On the nucleus structure and activity of comet 67P/Churyumov-Gerasimenko, *Science*, *347*(6220), AAA1044, doi:10.1126/science.aaa1044.

Sjogren, A., A. I. Eriksson, and C. M. Cully (2012), Simulation of potential measurements around a photoemitting spacecraft in a flowing plasma, *IEEE Trans. Plasma Sci.*, *40*, 1257–1261, doi:10.1109/TPS.2012.2186616.